Broadening of Molecular-Weight Distribution in Solid-State Polymerization Resulting from Condensate Diffusion

MICHAEL D. GOODNER,[1–3] STEPHEN M. GROSS,[1] JOSEPH M. DESIMONE,[1,2] GEORGE W. ROBERTS,[2] DOUGLAS J. KISEROW[1–3]

[1] Department of Chemistry, University of North Carolina, Chapel Hill, North Carolina 27599

[2] Department of Chemical Engineering, North Carolina State University, Raleigh, North Carolina 27695

[3] United States Army Research Office, Research Triangle Park, North Carolina 27709

Received 5 January 2000; accepted 20 May 2000

ABSTRACT: A kinetic model for the solid-state polymerization of poly(bisphenol A carbonate) in a single particle has been developed and used to investigate the broadening of molecular-weight distribution as a result of slow condensate diffusion. The model is based on melt-phase transesterification kinetics and Fickian diffusion of phenol, the condensate, in the amorphous regions of the semicrystalline particle. Model predictions compare favorably to experimental data. When diffusion is slow compared to reaction, a condensate concentration gradient is established. This gradient induces a molecular-weight gradient, which results in a broadened overall molecular-weight distribution with an overall polydispersity above the theoretical limit for homogenous step-growth polymerization. As the mass transfer resistance inside the particle is decreased, the average molecular weight increases faster with time, and the overall polydispersity decreases. A stoichiometric imbalance of end groups decreases the obtainable molecular weight but mitigates the deleterious effects of slow condensate diffusion. © 2000 John Wiley & Sons, Inc. J Appl Polym Sci 79: 928–943, 2001

Key words: diffusion; molecular-weight distribution; phenol; poly(bisphenol A carbonate); solid-state polymerization; stoichiometry

INTRODUCTION

Solid-state polymerization (SSP) is used to produce high-molecular-weight polymers suitable for a wide range of applications. For example, the poly(ethylene terephthalate) (PET) used in soft-drink bottles is produced exclusively through solid-state polymerization, and SSP provides PET and poly(butylene terephthalate) for several other applications.[1,2] High-grade, high-molecular-weight polyamides, including both nylon-6 and nylon-6,6, are also synthesized industrially through solid-state polymerization.[2,3] Recently, SSP has received attention as a possible technique for the formation of high-molecular-weight polycarbonates of bisphenol A,[4] potentially using supercritical carbon dioxide as a processing aid.[5,6]

Solid-state polymerization is employed industrially to avoid difficulties encountered in other polymerization processes. For example, melt-phase polymerizations of PET and polycarbonates cannot produce high-quality, high-molecular-weight polymer because high melt viscosities are encountered at even modest molecular weights. Increasing the processing temperature to reduce viscosity causes deleterious side reactions, such

Correspondence to: G. W. Roberts (groberts@eos.ncsu.edu).

Journal of Applied Polymer Science, Vol. 79, 928–943 (2001)

as the formation of color bodies in polycarbonates and acetaldehyde formation in the production of PET. Other polymerization processes (e.g., solution, suspension, and interfacial polymerization) have drawbacks, such as the generation of aqueous and/or organic waste streams.

In SSP, chips of relatively low-molecular-weight polymer (referred to as prepolymer) are partially crystallized, either thermally or through the action of a penetrant or nucleating agent. These chips are then heated to a temperature between the glass-transition temperature (T_g) of the amorphous polymer and the melting point (T_m) of the crystallites. The polymerization temperature must be above T_g to provide enough mobility for end groups to react. The temperature must be kept below T_m to prevent the crystallites from melting and thus allowing the particles to stick together.

A major consideration inherent in the SSP process is removal of the reaction byproduct, that is, the condensate, as polycondensation in general is a reversible reaction. Diffusion of the condensate in the individual polymer chips (internal diffusion) can be rate limiting. Removal of condensate from the solid-state reactor (external diffusion) can also be a limiting factor, and sweep fluids (primarily N_2) are employed to help strip the byproduct from the reactor.

Because of the industrial importance of SSP, many studies have focused on obtaining a better understanding of this process. An early attempt to describe SSP in single polymer particles considered only diffusion of the condensate and neglected reaction kinetics.[7] Recently, several research groups[8–10] have developed kinetic models for the solid-state polymerization of PET and have investigated the effects of condensate (ethylene glycol) diffusion on the molecular-weight evolution. Other aspects of the SSP of PET have also been examined, such as the effect of particle size,[9,11–14] the type of purge gas,[15] the flow rate of purge gas,[12–14] and the use of plasticizers to increase the rate of polycondensation.[6,13,16,17] Models for the SSP of nylon-6[3] and nylon-6,6[10] have also been developed. Solid-state polymerization in multiple particles and the effect of reactor type and conditions on the final product have also been examined for several different polymers.[3,18]

Broadening of the molecular-weight distribution (MWD), caused by slow diffusion of the condensate, is one general aspect of solid-state polymerization that has received relatively little attention. A condensate concentration gradient within the polymer particle produces a gradient in the local degree of polymerization because of the reversible nature of the step-growth reaction. At the particle surface the low concentration of the condensate allows the reaction to proceed further (i.e., to higher molecular weights) than in the interior of the particle, where the condensate concentration is higher. Such a gradient in molecular weight throughout the particle effectively broadens the molecular-weight distribution. Although the local polydispersity, that is, the ratio of the weight-average molecular weight to the number-average molecular weight, may be relatively low at each point in the particle, the polydispersity calculated over the entire particle will be greater and can exceed the theoretical limit of 2 for reversible step-growth polymerizations.[19] The existence of a molecular-weight gradient has been demonstrated in previous theoretical[8] and experimental[20] studies. However, the studies that have examined molecular-weight distribution in solid-state polymerization[13,21] have given only casual attention to the polydispersity values exceeding the theoretical limit.

Industrial interest in the SSP of polycarbonate is suggested by a large patent literature. However, few fundamental studies have been published. Iyer et al.[4] examined the feasibility of employing SSP to produce high-molecular-weight polycarbonates and studied the effect of polymerization time and temperature on the final molecular weight, crystallinity, and melting temperature. A subsequent study by the same research group examined the effect of SSP on the crystallite morphology of the resultant polymer.[22] Neither investigation reported the time rate of change of any of the polymer properties. In a recent study the temporal evolution of crystallinity, melting temperature, and molecular weight in polycarbonate SSP were examined using supercritical carbon dioxide as a crystallization aid.[5,6] To date, this is the only available information on polycarbonate SSP kinetics.

The synthesis of poly(bisphenol A carbonate) from bisphenol A and either phosgene or diphenyl carbonate is an $A_2 + B_2$ step-growth polymerization: the polymerization relies on reaction of two dissimilar monomers. The initial stoichiometry, *i.e.*, the initial molar ratio of the two monomers, has a pronounced effect on both molecular weight evolution and polydispersity. However, the impact of stoichiometry has not been considered in previous studies of SSP, which primarily focused

on PET, an A_2-type polymerization, and nylon-6, an A-B polymerization.

This article examines the broadening of the overall molecular-weight distribution in solid-state polymerization of poly(bisphenol A carbonate) through a combination of kinetic modeling and experimental investigation. Experimentally determined molecular weights at various times and at various locations in a single particle are compared with model predictions in order to establish reasonable values for three parameters in the model: the forward kinetic constant for polycondensation, the equilibrium constant, and the diffusion coefficient of the condensate, phenol. Then this model is used to investigate the effect of the phenol diffusion coefficient, the particle size, and the initial stoichiometric ratio of the two end groups. Although the results presented are for polycarbonate SSP, molecular-weight distribution broadening can occur in other systems. Therefore, the results provide a general insight into this aspect of solid-state polymerization.

EXPERIMENTAL

Prepolymer was produced by melt-phase transesterification of bisphenol A (BPA) and diphenyl carbonate (DPC) (both obtained from Aldrich, Milwaukee, Wisconsin) catalyzed by 300 ppm of lithium hydroxide monohydrate (Aldrich). The BPA was recrystallized from a methanol–water solution (1:1 by volume) and dried under vacuum at 60°C, while the DPC was recrystallized from hot methanol and dried under vacuum at room temperature. The catalyst was used as received and charged into the melt-phase reactor as an aqueous solution. Nitrogen was bubbled through the reactor to facilitate phenol removal. To compensate for DPC volatilization during the reaction, the DPC–BPA ratio in the charge to the reactor was 1.07:1 (mol:mol). Molecular-weight analyses were performed using gel-permeation chromatography. The prepolymer had a number-average molecular weight (M_n) of 1700 g/mol and a weight-average molecular weight (M_w) of 2500 g/mol. Thus, the polydispersity of the prepolymer was 1.4. At the end of the polymerization, the prepolymer was poured through a syringe into room-temperature water to form uniform beads, 3.6 mm in diameter with a mass of approximately 40 mg.

The prepolymer beads were crystallized by exposure to supercritical carbon dioxide as described by Gross et al.[5,6] For the beads used here, the average crystallinity after crystallization was 19 wt %, as determined by differential scanning calorimetry (DSC). Prepolymer beads crystallized to this value showed a uniform crystallinity throughout the particle.[6] Further details regarding the crystallization process and final morphologies may be found in Gross et al.[5,6]

Approximately 1 g of the semicrystalline beads was placed in the reactor, a steel vessel approximately 2 cm in diameter. Glass wool was used to support the beads in the center of the reactor, and N_2 was passed through the vessel. The reaction was carried out in four stages, each at a higher temperature. First the reactor was held at 180°C for 2 h after which 0.25 g of the beads was removed for analysis. The temperature of the reactor containing the remaining beads was increased to 205°C and held for another 2 h. Then another 0.25 g of the beads was removed. This process was repeated for the third and fourth stages of 2 h at 230°C and 6 h at 240°C.

The ramped temperature profile was used to take advantage of the higher polymerization rates afforded by an increase in the melting temperature of the crystallites as the polymerization proceeds.[5,6,22] The T_m of the crystallites was measured by DSC after each polymerization stage. The reactor temperature for the next stage was fixed just below this measured T_m to allow the highest rate of polymerization while avoiding particle agglomeration. Complete experimental details can be found in articles by Gross et al.[5,6]

Molecular weight was studied as a function of radial position in the particle as follows: a 0.4-mm-thick surface layer was shaved carefully off each of 10 beads using a razor blade. This process was repeated; this time a layer 1.0 mm thick was removed, leaving a 0.8 mm diameter core. Polymer from the 10 beads was then combined on a region-by-region basis, and the composite samples were analyzed to determine molecular weight. The three regions are hereafter referred to as the core (extending from the center to a radius of 0.4 mm), the middle (from 0.4 mm to 1.4 mm), and the shell (from 1.4 mm to the surface, 1.8 mm).

Model Development

Poly(bisphenol A carbonate) results from a transesterification reaction between hydroxyl and phenyl carbonate end groups to form a carbonate linkage and phenol. The reaction is:

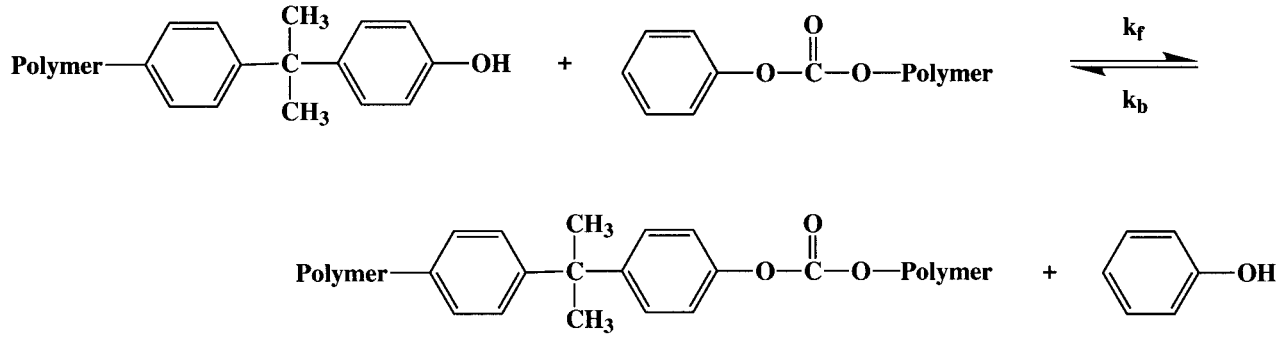

This reaction is reversible, so the byproduct, phenol, must be removed in order to achieve a high-molecular-weight polymer, that is, to minimize the effect of the reverse chain scission reaction. The equilibrium constant, K, for this reaction is defined by:

$$K \equiv \frac{k_f}{k_b} \tag{2}$$

where k_f is the kinetic constant for the polycondensation reaction and k_b is the kinetic constant for the chain scission reaction. The equilibrium constant for polytransesterification reactions is generally between 0.1 and 10,[19,23] and values reported for poly(bisphenol A carbonate) transesterification at temperatures between 150°C and 250°C range from 0.4 to more than 200.[24,25]

Leaving aside cyclic oligomers (the concentrations of which are low under normal polymerization conditions[26]), there are three linear species present in the polycarbonate particles:

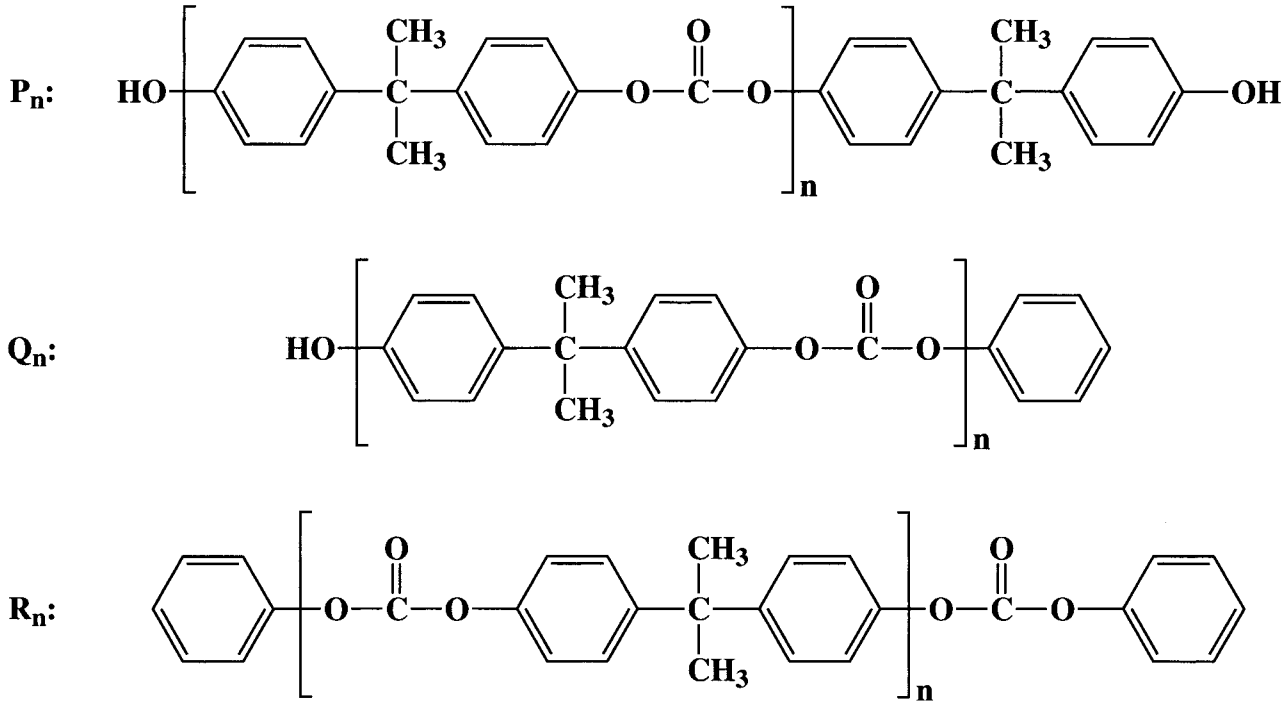

Thus, four different polycondensation reactions can occur:

$$P_n + R_m \leftrightarrow Q_{n+m+1} + C \tag{3}$$

$$P_n + Q_m \leftrightarrow P_{n+m} + C \tag{4}$$

$$R_n + Q_m \leftrightarrow R_{n+m} + C \tag{5}$$

$$Q_n + Q_m \leftrightarrow Q_{n+m} + C \tag{6}$$

where C denotes the condensate, phenol, and each reaction is assumed to have the same equilibrium constant and forward and reverse kinetic constants.

Models for the melt-phase transesterification of bisphenol A and diphenyl carbonate to form polycarbonate have been developed previously.[25,27] The successful adaptation of a melt-phase kinetic model to solid-state polycondensation has been demonstrated for the SSP of PET and of nylon-6,6.[10] A similar approach will be used here. The required assumptions are:

1. The polymer end groups and all small molecules, such as the condensate and catalyst, exist only in the amorphous regions of the semicrystalline particle. This assumption presumes these species are expelled from the developing crystallites during the crystallization process. This increase in concentration is represented by:

$$C_{\text{amorphous}} = \frac{C_{\text{total}}}{(1-f)} \tag{7}$$

   where f is the local crystalline weight fraction.
2. No reactions occur in the crystalline regions of the polymer since no reactive species (other than carbonate linkages) exist in the crystalline phase.
3. The effective condensate diffusivity is proportional to the amorphous fraction and the condensate diffusivity in the polymer melt:[28]

$$D^* = (1-f)D \tag{8}$$

   where D^* is the effective, observable diffusivity, and D is the diffusivity in the amorphous phase. Condensate diffusion occurs only through the amorphous regions. At low crystallinities (less than about 20%), crystallites should not obstruct significantly the diffusion of the condensate. However, at high crystallinity, the right side of eq. (8) must be divided by a tortuosity factor (>1) to compensate for the increased distance that the condensate molecule must travel to diffuse around the crystallites.
4. The transesterification reaction in the amorphous regions of the semicrystalline polymer proceeds in the same manner as a transesterification reaction occurring in a polymer melt at the same temperature. This assumption allows extant melt-phase kinetics to be applied to SSP.

Using the above assumptions, the melt-phase polycondensation model for polycarbonate developed by Kim and Choi[27] can be adapted to describe SSP in single polycarbonate pellets. That model is comprised of a system of 12 ordinary differential equations describing the temporal evolution of the moments of the species distributions for the polymeric species P_n, Q_n, and R_n. The kth moment of the distribution of P_n is given by

$$\lambda_{P,k} \equiv \sum_{n=1}^{\infty} n^k P_n \tag{9}$$

where P_n is the total concentration of species P_n (as opposed to number of moles in the Kim and Choi formulation). The moment equations for the distributions of Q_n and R_n are analogous. Note that the sums do not include the monomer concentrations P_0 and R_0 or the phenol concentration C, which is equivalent to Q_0. Also note that the total concentration is used in eq. (9) rather than in the amorphous-region concentration; this will lead to a factor of $1/(1-f)$ whenever the end-group concentration resulting from species P_n is required.

Species balances are written for the two monomers, phenol, and each distinct n-mer of each of the three polymeric species, producing an infinite set of equations because there are an infinite number of polymeric species. To reduce the number of equations, the concentrations of the polymeric species are transformed into moments using eq. (9), leaving 12 equations:

$$\frac{dP_0}{dt} = \frac{-2k_f}{(1-f)^2} P_0[2(\lambda_{R,0} + R_0) + \lambda_{Q,0}] + \frac{k_b C}{1-f}[\lambda_{Q,1} + 2\lambda_{P,0}] \tag{10}$$

$$R_C = \frac{k_f}{(1-f)^3}[4(\lambda_{P,0} + P_0)(\lambda_{R,0} + R_0) + 2(\lambda_{P,0} + \lambda_{R,0} + P_0 + R_0)\lambda_{Q,0} + \lambda_{Q,0}^2] - \frac{k_b C}{(1-f)^2}[2(\lambda_{P,1} + \lambda_{Q,1} + \lambda_{R,1}) - \lambda_{Q,0}] \tag{11}$$

$$\frac{dR_0}{dt} = \frac{-2k_f}{(1-f)^2} R_0[2(\lambda_{P,0} + P_0) + \lambda_{Q,0}] + \frac{k_b C}{1-f}[\lambda_{Q,1} + 2\lambda_{R,0}] \quad (12)$$

$$\frac{d\lambda_{P,0}}{dt} = \frac{2k_f}{(1-f)^2}[-2(\lambda_{R,0} + R_0)\lambda_{P,0} + \lambda_{Q,0}P_0] + \frac{k_b C}{1-f}[\lambda_{Q,1} - \lambda_{Q,0} - 2\lambda_{P,0}] \quad (13)$$

$$\frac{d\lambda_{Q,0}}{dt} = \frac{k_f}{(1-f)^2}[4(\lambda_{P,0} + P_0)(\lambda_{R,0} + R_0) - 2(\lambda_{P,0} + \lambda_{R,0} + P_0 + R_0)\lambda_{Q,0} - \lambda_{Q,0}^2] + \frac{k_b C}{1-f}[-\lambda_{Q,0} + 2(\lambda_{P,1} + \lambda_{R,1})] \quad (14)$$

$$\frac{d\lambda_{R,0}}{dt} = \frac{2k_f}{(1-f)^2}[-2(\lambda_{P,0} + P_0)\lambda_{R,0} + \lambda_{Q,0}R_0] + \frac{k_b C}{1-f}[\lambda_{Q,1} - \lambda_{Q,0} - 2\lambda_{R,0}] \quad (15)$$

$$\frac{d\lambda_{P,1}}{dt} = \frac{2k_f}{(1-f)^2}[-2(\lambda_{R,0} + R_0)\lambda_{P,1} + (\lambda_{P,0} + P_0)\lambda_{Q,1}] + \frac{1}{2}\frac{k_b C}{1-f}[\lambda_{Q,2} - \lambda_{Q,1} - 2(\lambda_{P,2} + \lambda_{P,1})] \quad (16)$$

$$\frac{d\lambda_{Q,1}}{dt} = \frac{2k_f}{(1-f)^2}[2(\lambda_{P,1} + \lambda_{P,0} + P_0)(\lambda_{R,1} + \lambda_{R,0} + R_0) - 2\lambda_{P,1}\lambda_{R,1} - (\lambda_{P,0} + \lambda_{R,0} + P_0 + R_0)\lambda_{Q,1}] + \frac{k_b C}{1-f}[\lambda_{P,2} + \lambda_{P,1} + \lambda_{R,2} + \lambda_{R,1} - \lambda_{Q,2}] \quad (17)$$

$$\frac{d\lambda_{R,1}}{dt} = \frac{2k_f}{(1-f)^2}[-2(\lambda_{P,0} + P_0)\lambda_{R,1} + (\lambda_{R,0} + R_0)\lambda_{Q,1}] + \frac{1}{2}\frac{k_b C}{1-f}[\lambda_{Q,2} - \lambda_{Q,1} - 2(\lambda_{R,2} + \lambda_{R,1})] \quad (18)$$

$$\frac{d\lambda_{P,2}}{dt} = \frac{2k_f}{(1-f)^2}[-2(\lambda_{R,0} + R_0)\lambda_{P,2} + (\lambda_{P,0} + P_0)\lambda_{Q,2} + 2\lambda_{P,1}\lambda_{Q,1}] + \frac{1}{6}\frac{k_b C}{1-f}[2\lambda_{Q,3} - 3\lambda_{Q,2} + \lambda_{Q,1} - 8\lambda_{P,3} - 6\lambda_{P,2} + 2\lambda_{P,1}] \quad (19)$$

$$\frac{d\lambda_{Q,2}}{dt} = \frac{2k_f}{(1-f)^2}[2\{(\lambda_{P,2} + \lambda_{P,1} + \lambda_{P,0} + P_0)(\lambda_{R,2} + \lambda_{R,1} + \lambda_{R,0} + R_0) - 2(\lambda_{P,2} + \lambda_{P,1})(\lambda_{R,2} + \lambda_{R,1}) + \lambda_{P,2}\lambda_{R,2}\} - (\lambda_{P,0} + \lambda_{R,0} + P_0 + R_0)\lambda_{Q,2} + \lambda_{Q,1}^2] + \frac{1}{3}\frac{k_b C}{1-f}[2\lambda_{P,3} + 3\lambda_{P,2} + \lambda_{P,1} - 4\lambda_{Q,3} + \lambda_{Q,1} + 2\lambda_{R,3} + 3\lambda_{R,2} + \lambda_{R,1}] \quad (20)$$

$$\frac{d\lambda_{R,2}}{dt} = \frac{2k_f}{(1-f)^2}[-2(\lambda_{P,0} + P_0)\lambda_{R,2} + (\lambda_{R,0} + R_0)\lambda_{Q,2} + 2\lambda_{R,1}\lambda_{Q,1}] + \frac{1}{6}\frac{k_b C}{1-f}[2\lambda_{Q,3} - 3\lambda_{Q,2} + \lambda_{Q,1} - 8\lambda_{R,3} - 6\lambda_{R,2} + 2\lambda_{R,1}] \quad (21)$$

In these equations C is the concentration of phenol in the amorphous phase, and P_0 and R_0 are the total concentrations of the bisphenol A and diphenyl carbonate monomers, respectively.

The implicit assumption of a constant crystalline fraction is contained in Eqs. (10)–(21). However, it is known that further crystallization may occur during the solid-state polymerization of polycarbonate[4–6,22] and that a crystallinity gradient may be established between the high- and low-molecular-weight regions.[6] Unfortunately, the evolution of crystallinity during SSP, as well as its dependence on various process and physicochemical parameters (molecular weight, temperature, etc.), has not been characterized quantitatively. Therefore, it is not practical to incorporate the effect of changing crystallinity into the SSP model at the present time. The assumption of constant crystallinity will be given additional consideration in the next section.

Because polymerization is reversible (i.e., longer polymer chains can be cleaved into shorter ones), the differential equations representing the rate of change in the kth moment of a distribution are dependent on the k + 1th moment. Therefore, a closure rule is required to cast the k + 1th moment in terms of the lower order moments. For reversible polymerizations a suitable formula, originally developed in a study of reversibly agglomerating particles,[29] was adopted by Tai et al.[30]:

$$\lambda_{i,3} = \frac{2\lambda_{i,0}\lambda_{i,2}^2 - \lambda_{i,1}^2\lambda_{i,2}}{\lambda_{i,0}\lambda_{i,1}} \quad (22)$$

where i can be either P, Q, or R.

The number- and weight-average molecular weights can be expressed in terms of the moments of the individual species' concentration distributions. Denoting the molecular weight of a molecule P_n to be W_{Pn}, the total zeroth, first, and second moments of the molecular weight distribution are calculated from

$$\mu_0 = \sum_{n=1}^{\infty} (P_n + Q_n + R_n) + P_0 + R_0$$
$$= \lambda_{P,0} + \lambda_{Q,0} + \lambda_{R,0} + P_0 + R_0 \quad (23)$$

$$\mu_1 = \sum_{n=}^{\infty} (P_n W_{P_n} + Q_n W_{Q_n} + R_n W_{R_n}) + P_0 W_{P_0}$$
$$+ R_0 W_{R_0} = M_r(\lambda_{P,1} + \lambda_{Q,1} + \lambda_{R,1})$$
$$+ M_P(\lambda_{P,0} + P_0) + M_Q\lambda_{Q,0} + M_R(\lambda_{R,0} + R_0) \quad (24)$$

$$\mu_2 = \sum_{n=1}^{\infty} (P_n W_{P_n}^2 + Q_n W_{Q_n}^2 + R_n W_{R_n}^2) + P_0 W_{P_n}^2$$
$$+ R_0 W_{R_n}^2 = M_r^2(\lambda_{P,2} + \lambda_{Q,2} + \lambda_{R,2})$$
$$+ 2M_r(M_P\lambda_{P,1} + M_Q\lambda_{Q,1} + M_R\lambda_{R,1})$$
$$+ M_P^2(\lambda_{P,0} + P_0) + M_Q^2\lambda_{Q,0} + M_R^2(\lambda_{R,0} + R_0) \quad (25)$$

In eqs. (23)–(25), M_r represents the molecular weight of a structural repeat unit, and M_P, M_Q, and M_R are the molecular weights of bisphenol A, phenol, and diphenyl carbonate, respectively. The number-average molecular weight (M_n), weight-average molecular weight (M_w), and polydispersity index (PDI) are given by

$$M_n = \frac{\mu_1}{\mu_0} \quad (26)$$

$$M_w = \frac{\mu_2}{\mu_1} \quad (27)$$

$$\mathrm{PDI} = \frac{M_w}{M_n} = \frac{\mu_2\mu_0}{\mu_1^2} \quad (28)$$

To complete the solution of eqs. (10)–(28), the phenol concentration (C) must be calculated as a function of time and position in the particle. This is accomplished by writing a mass balance for phenol that includes diffusion in the polycarbonate bead. Assuming that diffusion in the amorphous regions of the semicrystalline particles is Fickian, this balance reads

$$\frac{\partial}{\partial t}[(1 - f)C] = R_C + \nabla \cdot (D^*\nabla C) \quad (29)$$

The term on the left-hand side represents the time rate of change of the *total* phenol concentration. The first term on the right-hand side is the net generation rate of phenol by the transesterification process, which is given by the right-hand side of eq. (11). The second term describes the net rate of diffusion.

The method of lines was used to solve eqs. (10), (12)–(21), and (29). The computational domain representing the spherical polymer bead was divided into 51 grid points spaced equidistant along the radius, with point 1 at the center of the bead and point 51 at the surface. The number of divisions was varied to verify that using more points did not provide any appreciable gains in numerical accuracy. The spatial derivative in eq. (29) was discretized using a centered second-order finite difference, and the resulting system of (51 $\times$ 12) ordinary differential equations was solved using a commercial numerical integration package for solving stiff sets of differential equations (NAG Fortran Library, Mark 18, Numerical Algorithms Group; Oxford, United Kingdom). The values of D, k_f, and k_b were assumed to be independent of time and position, corresponding to an isothermal particle, and the value of f also was assumed to be independent of time and position.

To solve the set of equations, boundary conditions on the phenol concentration and initial conditions for the 12 dependent variables are required. The boundary conditions applied at the particle center and surface are

$$\left.\frac{\partial C}{\partial r}\right|_{r=0} = 0 \quad (30)$$

$$C_{r=d/2} = 0 \quad (31)$$

The boundary condition at the particle center is required by symmetry. A zero phenol concentration at the particle surface results from the as-

Table I Initial Conditions and Physicochemical and System Parameters Used in Single-Particle Kinetic Model

Initial Conditions for Monomer and Phenol Concentration		
$P_0 = 0$ mol/L	$C = 0$ mol/L	$R_0 = 0$ mol/L
Initial Conditions for the Species Concentration Moments		
$\lambda_{P,0} = 0.102$ mol/L	$\lambda_{Q,0} = 0.205$ mol/L	$\lambda_{R,0} = 0.102$ mol/L
$\lambda_{P,1} = 0.627$ mol/L	$\lambda_{Q,1} = 1.25$ mol/L	$\lambda_{R,1} = 0.627$ mol/L
$\lambda_{P,2} = 6.16$ mol/L	$\lambda_{Q,2} = 12.3$ mol/L	$\lambda_{R,2} = 6.16$ mol/L
Physicochemical and System Parameters		
$k_f = 3.0 \times 10^{-2}$ L mol^{-1} min^{-1}	$k_b = 1.0 \times 10^{-3}$ L mol^{-1} min^{-1}	$K = 30$
$D = 1 \times 10^{-7}$ cm^2/s	$d = 3.6$ mm	

sumptions that: (1) mass transfer from the surface of the particle to the sweep fluid is rapid, that is, the mass transfer coefficient is infinite; and (2) the phenol concentration in the sweep gas is 0.

The initial conditions were calculated to give initial values of M_n and M_w equal to 1750 and 2500, respectively, that is, the molecular weights of the prepolymer in the SSP experiments. The initial concentrations of monomers and phenol in the prepolymer were assumed to be 0. This is reasonable since these molecules should have been extracted effectively from the polymer particles during the crystallization step carried out in supercritical CO_2.

For a prepolymer with stoichiometrically balanced end groups, the moments of the individual species distributions are related through

$$\lambda_{P,k} = \tfrac{1}{2}\lambda_{Q,k} = \lambda_{R,k} \tag{32}$$

This equation represents the most probable distribution. This leaves three independent moments (one each of the zeroth, first, and second moments) to be determined at time 0. Two pieces of data, the number- and weight-average molecular weights, are available. The third piece of data arises from conservation of monomer moieties during the polymerization, that is, 2.7M for bisphenol A in a 1:1 molar mixture with diphenyl carbonate. This value can be related to the zeroth and first moments of the species distributions:

$$P_0 + \lambda_{P,1} + \lambda_{P,0} + \lambda_{Q,1} + \lambda_{R,1} = constant \tag{33}$$

or, upon substitution:

$$4\lambda_{P,1} + \lambda_{P,0} = 2.7 \tag{34}$$

Thus, the initial values of the moments can be calculated. The values used in the simulation are found in Table I.

To simulate the SSP of stoichiometrically unbalanced prepolymer, a different procedure was used to determine the initial values of the moments. A homogeneous melt-phase polymerization of bisphenol A with excess diphenyl carbonate was simulated by setting the crystalline fraction to 0 and making the phenol diffusion coefficient arbitrarily high. The resulting values of the moments that correspond to a number-average degree of polymerization of 10 then were used for the initial conditions for the SSP simulations.

Number- and weight-average molecular weights were calculated at each of the 51 spatial grid points. The simulated spherical pellet was divided into 51 corresponding shells, and the volume fraction of each of these shells was computed. Because the polymer crystalline fraction is assumed invariant both spatially and temporally, volume fraction and weight fraction are equivalent. The weight fractions were then used to calculate the average molecular weights for the entire particle using existing formulae for computation of average M_n and M_w values for mixtures of polymers having different molecular-weight distributions[19]:

$$\overline{M}_n = \frac{1}{\sum_i \frac{w_i}{M_{n,i}}} \tag{35}$$

$$\overline{M}_w = \sum_i w_i M_{w,i} \tag{36}$$

In these equations w_i is the weight fraction of polymer corresponding to grid point i, and $M_{n,i}$

and $M_{w,i}$ are, respectively, the number- and weight-average molecular weights at that grid point. The average molecular weights for the entire particle are referred to as *overall* molecular weights.

Several system and physicochemical parameters are required to apply the above model. A complete set of the values used in the following calculations is presented in Table I. Three significant assumptions/estimates were made because reliable data for the polycarbonate system was not available:

1. The crystalline fraction does not vary with time or radial position in the particle. Although SSP studies have shown that crystallinity increases during polymerization,[4,5,22] the assumption of constant crystallinity is necessary in the absence of a sound model for the kinetics of crystallization caused by solid-state reactions. The crystallinity was fixed at 20 wt %, close to the value of 19% for the crystallized prepolymer.
2. The phenol diffusion coefficient in the amorphous phase (D) initially was set at 1×10^{-7} cm^2/s, although the effect of changing this value was studied later. No values for the diffusivity of phenol in polycarbonate were found in the literature, although the diffusivities of deuterated methanol and perdeuterated acetone in *glassy* polycarbonate at room temperature were reported to be 10^{-9} and 10^{-6} cm^2/s, respectively.[31] Therefore, there is significant uncertainty about the value of the phenol diffusivity used in this study. In fact, there is significant uncertainty about the diffusivity for even the more common ethylene glycol–PET system. The reported values of the diffusion coefficient of ethylene glycol in PET differ by 2 to 3 orders of magnitude in the region of 250°C.[10,28,32–35]
3. The rate constants k_f and k_b, and therefore the equilibrium constant (K), were fixed over the course of the reaction, even though the temperature was changed during the experimental polymerization. This assumption simplifies the mathematics and is necessary because no reliable data exist on the kinetics of polycarbonate transesterification in the open literature, although there is some published data for this reaction.[24,25] It can be inferred from the values of the equilibrium constants determined in those studies that an exothermic reaction occurs when no catalyst is present, but an endothermic reaction happens when lithium hydroxide monohydrate is used as a catalyst, behavior that is thermodynamically inconsistent. The process for choosing the chain scission kinetic constant, k_b, and the kinetic constant for polycondensation, k_f, is described in the discussion of Figure 1.
4. Phenol diffusivity also was held constant over the course of the reaction, even though the temperature was varied. Thus, the assumed diffusivity value represents an approximate average over the temperature range studied. In view of the lack of any data on the diffusivity of phenol in polycarbonate, it obviously was not possible to estimate *a priori* the temperature dependence of the phenol diffusion coefficient.

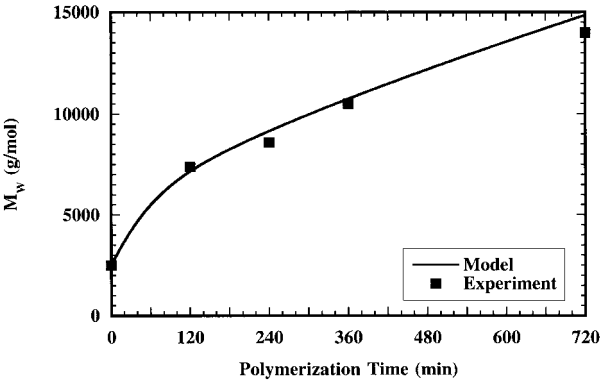

Figure 1 Comparison of experimental and simulated overall weight-average molecular weights for solid-state polymerization of polycarbonates. The values used in the model are listed in Table I.

RESULTS AND DISCUSSION

Comparison of Model with Experiment

Figure 1 compares the overall weight-average molecular weight (M_w) predicted by the kinetic model to that of the experimental results. The forward rate constant for the transesterification reaction (k_f) was adjusted to give the best agreement between the experimental data and the model predictions. With the values of the phenol diffusion coefficient (D) and the chain scission rate constant (k_b) shown in Table I, the model described the first few data points in Figure 1

reasonably well, as long as the value of k_f was such that the value of the equilibrium constant (K) was on the order of those reported in the literature.[24,25] However, the agreement between the data and the model at longer reaction times was much more sensitive to the value of k_f. The best qualitative agreement with the experimental data for molecular weight evolution was provided by $k_f = 3.0 \times 10^{-2}$ L mol^{-1} min^{-1}. Thus, k_f was fixed at this value, giving a K of 30. This value is within the range reported.[24,25]

The model predictions mimic the experimental data quite well. Although true values for the physicochemical parameters (K, k_f, and D) cannot be determined from this exercise, the formulation used for the kinetic model does reproduce the measured molecular weight evolution to within the accuracy of the experimental measurements ($\pm$1000 g/mol).

During the first hour of polymerization, the rate of increase of the molecular weight was relatively high. This is a direct result of the equilibrium nature of the polymerization. During the crystallization step, most remaining phenol from the melt transesterification was removed from the prepolymer. Therefore, in the initial stage of SSP, the transesterification reaction is far from equilibrium, and the end-group concentrations are high. Chain scission is infrequent and molecular weight increases rapidly. Between 1 and 2 h of polymerization time, the rate of molecular-weight increase declines. The phenol produced during the initial stage of reaction begins to accumulate in the particle, and it limits the molecular-weight increase due to equilibrium.

The equilibrium nature of polycarbonate polycondensation is displayed more clearly in Figure 2. Calculated phenol concentrations in the particle are shown in Figure 2(a). During the first hour of polymerization the polycondensation reaction causes a quick buildup of phenol from its initial zero concentration. Near the surface of the particle phenol removal is relatively rapid, and the concentration in this region ($d/2 \geq 0.15$ cm) begins to decline after about the first hour of polymerization. In the center of the particle the phenol concentration is high (well above 0.2M) and continues to increase for several hours. These high concentrations limit the molecular weight through increased chain scission, leading to a radial gradient in molecular weight throughout the particle.

Figure 2(b) shows model predictions of molecular-weight evolution at several locations in the particle. Toward the surface (r = 1.62 mm curve), the rate of molecular-weight increase declines with time but still proceeds at a satisfactory rate because phenol concentration is low. However, in

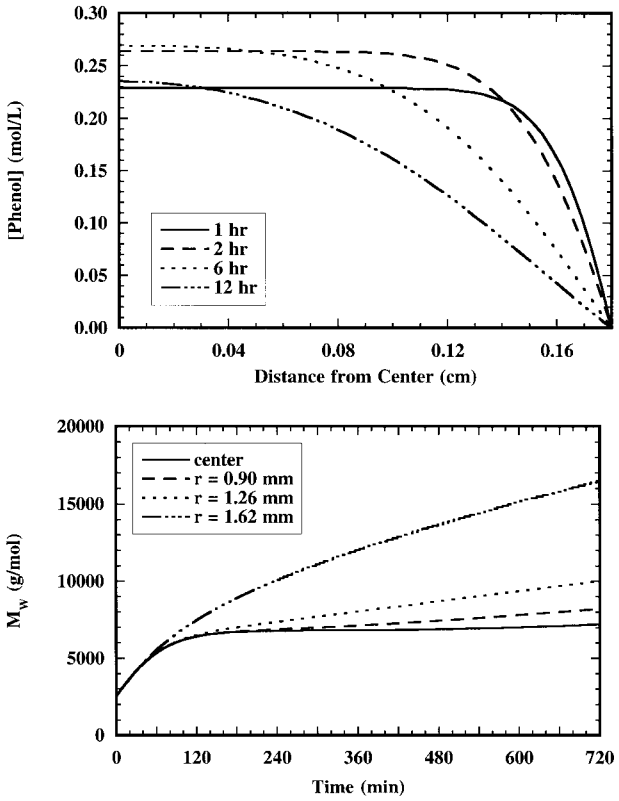

Figure 2 For the polymer bead for the simulated polymerization shown in Figure 1: (a) phenol concentration in amorphous region; and (b) local molecular weight at various positions.

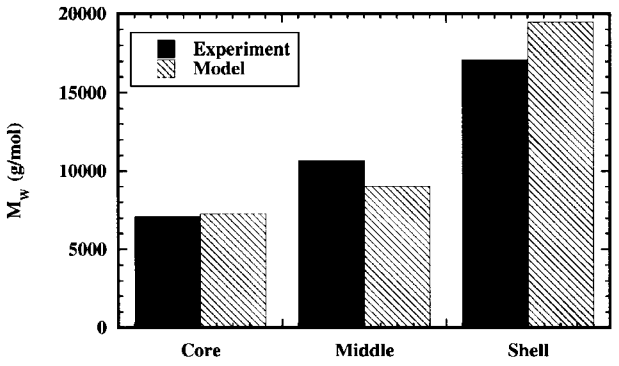

Figure 3 Comparison of experimental and simulated average M_w's for the core, middle, and shell regions after 12 hours polymerization. The core region extends from the center of the particle to a radial position of 0.4 mm, the middle from 0.4 mm to 1.4 mm, and the shell from 1.4 mm to the surface, 1.8 mm.

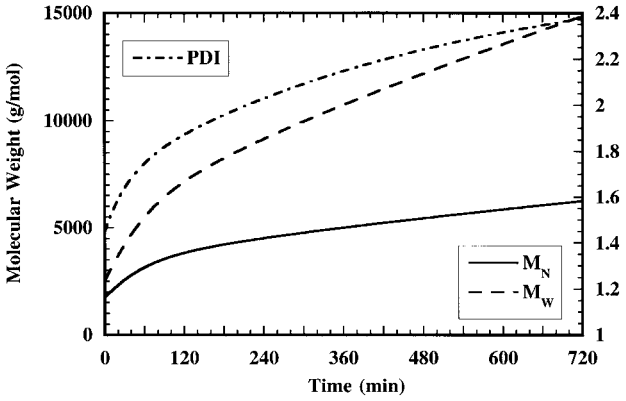

Figure 4 Overall average molecular weights and overall polydispersity for the simulated polymerization in Figure 1. The polydispersity is M_w/M_n.

the particle interior, polymerization nearly ceases because the equilibrium concentration of phenol is reached. After 720 min the M_w in the center of the particle is approximately a factor of 2.5 lower than the M_w near the surface (r = 1.62 mm).

Figure 3 compares model predictions to experimentally determined molecular weights after 12 h of SSP for the core, middle, and shell regions, as defined in the experimental section. The agreement is very good, especially given that the adjustable parameter in the model, k_f, was used to fit only the *overall* molecular-weight data in Figure 1, without considering the local M_w values.

The molecular-weight gradient caused by slow phenol diffusion can affect the processing characteristics of the polymer. The broadening of the molecular-weight distribution, as represented by the polydispersity index, is shown in Figure 4. In an ideal, homogeneous system, polydispersities for reversible step-growth polymerizations do not exceed a theoretical limit of 2. In solid-state polymerization, however, when the gradients in phenol concentration and molecular weight are pronounced, polydispersities can exceed the theoretical limit. For example, under the conditions simulated, the PDI rises above 2 after 210 min of polymerization, when the overall M_w is only about 8000 g/mol, and is nearly 2.4 after 720 min ($M_w \simeq$ 15,000 g/mol). In the experimental studies the final polydispersity was approximately 2.4 at an overall M_w of about 15,000 g/mol.

Parametric Investigation of Solid-State Polymerization

Several series of simulations were run to understand better the conditions under which molecular-weight distribution broadening occurs. In the first series the effect of the phenol diffusion coefficient was examined. The results are shown in Figure 5. Over the first hour of the reaction, the value of the diffusion coefficient is not important within the range of parameters studied, as the average molecular weight [Fig. 5(a)] and polydispersity [Fig. 5(b)] profiles are nearly independent of the value of D. During this stage phenol concentration is low and only beginning to build up, so that the frequency of chain scission is insignificant. After 1 h the phenol concentration begins to have an effect on polymerization. When the diffusion coefficient is low (10^{-7} to 10^{-6} cm^2/s), phenol concentration in the particle is high, and reaction slows down considerably. In fact, the molecular-weight and polydispersity profiles for the two smallest diffusion coefficients (5×10^{-8} and 1×10^{-7} cm^2/s) follow nearly the same path. Polymerization has all but ceased throughout most of

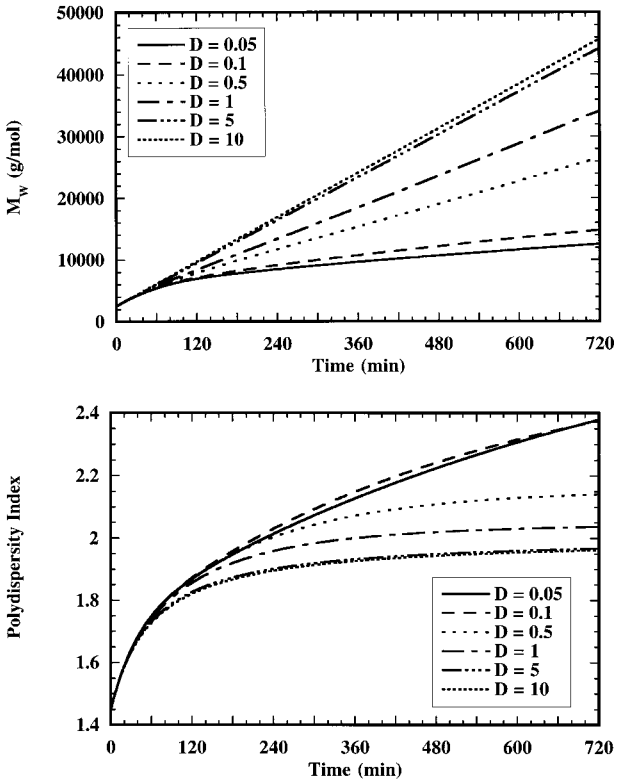

Figure 5 (a) Effect of phenol diffusion coefficient on the overall M_w predicted by the kinetic model. The values of the diffusion coefficient in the legend have been multiplied by 10^6 (i.e., D = 0.1 corresponds to 1.0 $\times 10^{-7}$ cm^2/s). The values of the other parameters are listed in Table I (b) Polydispersities predicted by the kinetic model for the polymerization shown in Figure 5 (a).

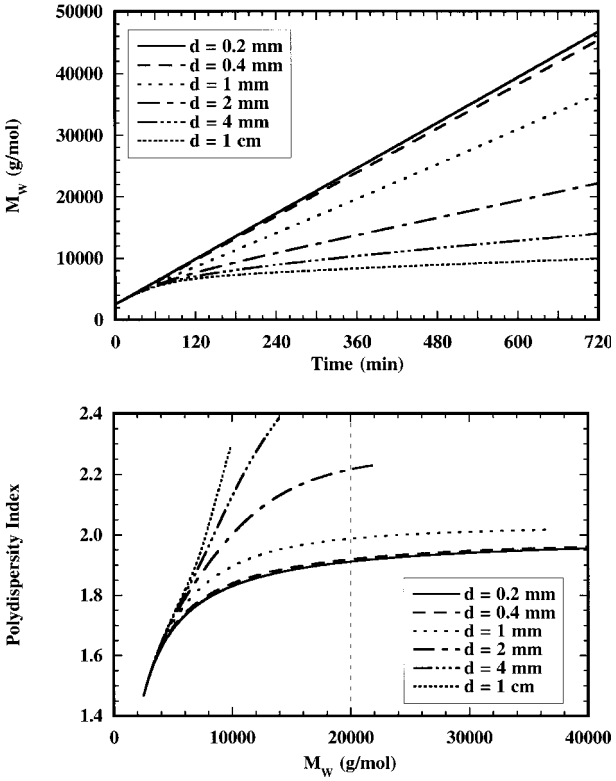

Figure 6 (a) Effect of particle size on overall M_w as predicted by the kinetic model—particle diameter denoted by d; the values of other parameters are listed in Table I; (b) Profiles of polydispersities versus average M_w for the predictions shown in Figure 6 (a). The vertical line indicates an average M_w of 20,000 g/mol; the times required to reach this threshold are shown in Table II, along with the corresponding polydispersity values.

the particle. Only a small molecular-weight increase near the surface of the pellets causes the overall average molecular weight to increase. For the lowest values of the diffusion coefficient, the polydispersity exceeds the theoretical limit of 2 only 3 h into the reaction and continues to increase with time. As the diffusion coefficient is increased, the rate of molecular-weight buildup increases, and the final polydispersities decrease, although the final PDI is still above 2 for a diffusivity of 10^{-6} cm^2/s. For the highest values studied (5×10^{-6} and 1×10^{-5} cm^2/s), the molecular-weight and polydispersity profiles become nearly coincident, with the molecular weight increasing linearly with time and the polydispersity approaching an asymptote of 2. These features indicate that the intrinsic kinetics of the polycondensation reaction have become the limiting factor, as phenol removal is sufficiently fast to eliminate any appreciable chain scission. The rate of reaction is nearly constant throughout the particle, and the overall molecular weight is equal to the local molecular weight at each position.

For the conditions simulated, the rate of overall molecular-weight increase will be greater and final polydispersity will be lower if the diffusivity of the condensate can be increased. Raising the temperature will increase the diffusion coefficient somewhat, but this approach is limited by the T_m (maximum temperature) for solid-state polymerization. In addition, raising the temperature may be counterproductive if K decreases or k_f increases more rapidly than D. A more elegant method of raising the condensate diffusivity is to introduce a plasticizing agent, which will effectively increase the free volume of the polymer and consequently enhance molecular mobility and increase the diffusion coefficient.[6,13,16,17] Of particular interest are nontoxic penetrants such as supercritical carbon dioxide, which plasticize the polymer without contaminating it or generating difficult-to-recycle waste streams.[5,6]

Figure 6(a,b) shows the effect of particle size on average molecular weight and polydispersity for a phenol diffusion coefficient of 10^{-7} cm^2/s. As the particle size is increased, diffusional limitations become more pronounced. Very small particles (less than 0.4 mm in diameter) show essentially no diffusional influence, and the rate of molecular-weight increase is constant. However, particles of even intermediate sizes (e.g., 1–2 mm in diameter) show a significantly lower overall average molecular weight at any time because of condensate buildup in the particle interior. The largest particle considered (1 cm in diameter) showed only a negligible increase in average molecular weight after the initial period of phenol buildup.

Table II Polymerization Time Required to Reach an Average M_w of 20,000 g/mol for Model Predictions Shown in Figure 6(b)

Particle Diameter (mm)	Polymerization Time (min)	Polydispersity Index
0.2	285	1.91
0.4	294	1.92
1	369	1.99
2	628	2.22
4	1610	2.44
10	8590	2.52

The polydispersities are also listed.

Polydispersity as a function of molecular weight is depicted in Figure 6(b). The smallest particles show the lowest polydispersities for a given molecular weight, and the PDI values appear to approach the theoretical limit of 2 asymptotically at high molecular weights. For larger particles, in which mass transfer limitations are important, polydispersities are much higher.

Table II shows the times required to reach an overall average M_w of 20,000 g/mol and the polydispersities at this molecular weight as a function of particle size. Two deleterious effects stemming from mass transfer limitations appear as the particle size is increased: (1) the time required to reach a given molecular weight increases dramatically; and (2) the polydispersity of the polymer increases. From a purely kinetic viewpoint, small particles, that is, powders, are the most desirable form for the polycarbonate prepolymer.

Stoichiometry can also have a significant effect on the evolution of the overall molecular weight and its distribution. Loss of diphenyl carbonate during the melt-phase formation of prepolymer can be significant because of the low boiling point of DPC.[27] Side reactions can also change the end-group ratio, such as the hydroxyl-catalyzed degradation of bisphenol A end groups to unreactive color bodies.[36] To investigate the polymerization behavior when phenyl carbonate and hydroxyl end groups are not present in stoichiometric balance, a series of simulations was performed. The stoichiometric excess is defined here as the molar percent excess of one type of end group initially present in the monomer from which the prepolymer is synthesized. For example, a prepolymer synthesized from a monomer mixture consisting of 1.05 mol diphenyl carbonate per 1 mol bisphenol A would have a 5% stoichiometric excess. For this series of simulations, 3 stoichiometric excesses are examined (2%, 5%, and 10%), all with a starting M_n of 1270 g/mol for the prepolymer (corresponding to a degree of polymerization of 10). Monomer evaporation and side reactions of the end groups during SSP were not considered in this study.

Figure 7(a) shows the influence of stoichiometric excess on the overall weight-average molecular weight for parameter values that lead to radial gradients in phenol concentration and molecular weight. When the end groups are present in equal amounts, the highest rate of molecular-weight increase is achieved. Increasing the stoichiometric excess decreases the rate of polymerization and the final molecular weight. Figure

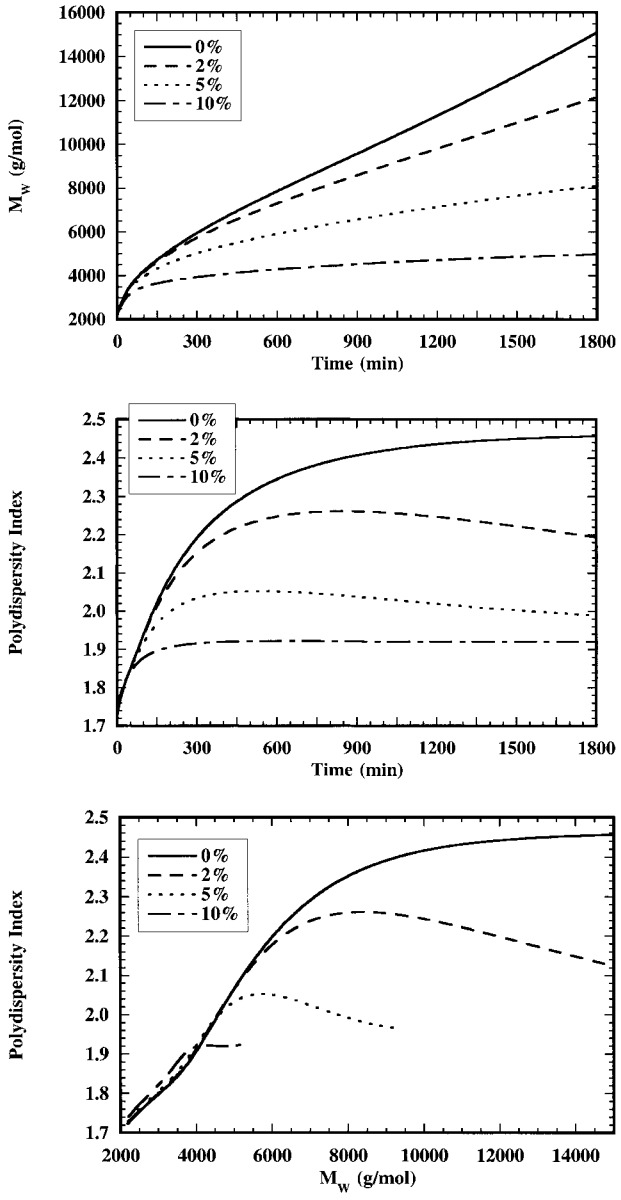

Figure 7 (a) Effect of stoichiometric excess on the overall M_w, as predicted by the kinetic model—percent stoichiometric excess and initial conditions are defined in the text; all other parameters listed in Table I; (b) Polydispersities (PDIs) versus time and stoichiometric excess for the simulation shown in Figure 7 (a); (c) PDIs as a function of stoichiometric excess and average M_w for the predictions shown in Figure 7 (a).

7(b) shows that the overall polydispersity decreases as the stoichiometric excess is increased. As the rate of polymerization decreases due to the nonstoichiometric ratio of end groups, more time is available for phenol removal from the polymer particles, and the concentration gradients become less severe. For a given stoichiometric excess,

polydispersities initially increase, go through a maximum, and then begin to decrease over the course of the reaction. Initially, the polymerization is mass transfer limited throughout the entire particle, and a phenol gradient arises, which causes a molecular-weight gradient and a broadened molecular-weight distribution. However, when an $A_2 + B_2$ polymerization (such as polycarbonate synthesis) is performed, there is a maximum obtainable molecular weight, which decreases with increasing stoichiometric imbalance. As the shell region of the particle approaches this molecular weight, the rate of polymerization in this region approaches 0, allowing the interior regions to "catch up." In this manner, the phenol and molecular-weight gradients inside the particle are diminished, leading to a reduction in the polydispersity over the remainder of the reaction.

Figure 7(c) shows the polydispersity as a function of overall weight-average molecular weight and stoichiometric excess and suggests a possible operating paradigm for polydispersity control in SSP. If a less polydisperse material is needed and reducing the particle size is not an option, stoichiometry may be used to mitigate the adverse effects of slow mass transfer. For example, if polymer having an M_w of 14,000 g/mol and a polydispersity below 2.2 is desired, a polymerization may be performed on prepolymer synthesized from a monomer mixture having a 2% stoichiometric excess of either monomer. Although the polymerization takes longer with a stoichiometric imbalance, reduced polydispersities may be obtained without resorting to intensive postprocessing.

Model Assumptions

When applied to the SSP of poly(bisphenol A carbonate), the present model requires several assumptions that limit its utility as a predictive tool. The most important of these assumptions are: (1) the values of k_f, K (or k_b), and D are known at some temperature; (2) the percentage of crystalline material does not change during polymerization; and (3) the effect of temperature on k_f, K, and k_b can be neglected. The last two assumptions are not valid generally and would have to be removed in a more rigorous version of the model. For example, for the polymerization shown in Figure 3, the percent crystallinity increased from the initial value of 19% to approximately 50% in the shell region, although there was no appreciable increase in the core region despite the modest molecular-weight increase. This increase in crystallinity lowers D^*, as shown by eq. (8), and increases the concentration of end groups in the amorphous region, as shown by eq. (7).

Assumptions 2 and 3 are believed to be justified currently because accurate values of k_f, K, and D are not available. In fact, the values of these parameters used in the preceding calculations probably are accurate only to about an order of magnitude. Therefore, the uncertainty introduced by using the values of these parameters shown in Table I at some "average" polymerization temperature probably is far greater than the uncertainties introduced by the second and third assumptions. Moreover, to remove these two assumptions, an additional set of information would have to be available, that is, activation energies for D and k_f, the enthalpy of reaction, and a relationship between percent crystallinity and the process parameters that control SSP and/or between the percent crystallinities and the polymer properties. This kind of information is not available currently.

Despite these quantitative limitations the present model is able to provide a very useful qualitative perspective concerning the SSP of poly(bisphenol A carbonate) and, in particular, the broadening of the molecular-weight distribution that occurs when internal transport of the condensate molecule is slow.

CONCLUSIONS

The broadening of the molecular-weight distribution in the SSP of poly(bisphenol A carbonate) has been studied using both experimental and modeling techniques. A kinetic model describing the molecular-weight evolution throughout spherical polymer beads is developed, and its predictions are compared to experimental SSP data. The model was fit to the experimental data by adjusting the transesterification rate constant (k_f) to match measurements of the overall average molecular weight versus the polymerization time. Good agreement was obtained, not only for the temporal evolution of the molecular weight but also for the final molecular weights in the core, middle, and shell regions of the particle. The experimental data show a significant radial molecular-weight gradient within the polymeric bead. The model was used to identify the slow removal of the condensate (phenol) as the probable cause of this molecular-weight gradient. The molecular-

weight gradient in the particle leads to broadening in the overall molecular-weight distribution.

The model was used to investigate the effect of three parameters on the average molecular weight and the polydispersity: (1) the phenol diffusion coefficient, D; (2) the particle size; and (3) the stoichiometric excess of end groups in the prepolymer. The diffusion coefficient and the particle size have similar effects on the final average molecular weight. As the internal mass transfer resistance is decreased by increasing the phenol diffusivity and/or decreasing the particle size, the rate of overall molecular-weight increase is increased and the polydispersity is decreased. Increasing the stoichiometric excess of one of the end groups decreases the rate of polymerization. However, the polydispersity of the final polymer is also decreased.

This work was performed while one author (M.D.G.) held a National Research Council–U.S. Army Research Office research associateship. The authors would also like to thank the U.S. Army Research Office for funding and the Kenan Center for the Utilization of Carbon Dioxide for additional support.

NOMENCLATURE

- C phenol concentration in *amorphous* phase (mol/L)
- d polymer bead diameter (mm)
- D phenol diffusivity in amorphous polycarbonate (cm^2/s)
- D^* effective phenol diffusivity; defined by eq. (8) (cm^2/s)
- f local weight fraction crystallinity
- K transesterification equilibrium constant
- k_b reverse (chain scission) kinetic constant ($L\ mol^{-1}\ min^{-1}$)
- k_f forward (transesterification) kinetic constant ($L\ mol^{-1}\ min^{-1}$)
- M_n number-average molecular weight (g/mol)
- M_P molecular weight of bisphenol A (228.3 g/mol)
- M_r molecular weight of polycarbonate repeat unit (254.3 g/mol)
- M_R molecular weight of diphenyl carbonate (214.2 g/mol)
- M_Q molecular weight of phenol (94.1 g/mol)
- M_w weight-average molecular weight (g/mol)
- P_n dihydroxyl-terminated polymer of n repeat units; symbol represents both species and its total concentration (mol/L)
- Q_n polymer of n repeat units having 1 hydroxyl and 1 phenyl carbonate end group; symbol represents both species and its total concentration (mol/L)
- R_C rate of production of condensate due to reaction, as given by eq. (11)
- R_n diphenyl carbonate terminated polymer of n repeat units; symbol represents both species and its total concentration (mol/L)
- W_{Pn} molecular weight of species $P_n = n \cdot M_r + M_P$ (g/mol)
- W_{Qn} molecular weight of species $Q_n = n \cdot M_r + M_Q$ (g/mol)
- W_{Rn} molecular weight of species $R_n = n \cdot M_r + M_R$ (g/mol)
- $\lambda_{X,k}$ kth moment of concentration distribution of species X (mol/L)
- μ_k kth moment of overall molecular-weight distribution (g^{k-1}/mol^{k-1})

REFERENCES

1. Gostoli, C.; Pilati, F.; Sarti, G. C.; DiGiacomo, B. J Appl Polym Sci 1984, 29, 2873.
2. Pilati, F. In Comprehensive Polymer Science; Bevington, J. C., Allen, G. C., Eds.; Pergamon: Oxford, UK, 1989; Vol. 5, p 201.
3. Plazl, I. Ind Eng Chem Res 1998, 37, 929.
4. Iyer, V. S.; Sehra, J. C.; Ravindranath, K.; Sivaram, S. Macromolecules 1993, 26, 1186.
5. Gross, S. M.; Flowers, D.; Roberts, G.; Kiserow, D. J.; DeSimone, J. M. Macromolecules 1999, 32, 3167.
6. Gross, S. M.; Roberts, G. W.; Kiserow, D. J.; DeSimone, J. M. Macromolecules 2000, 33, 40.
7. Chen, F. C.; Griskey, R. G.; Beyer, G. H. AIChE J 1969, 15, 680.
8. Zhi-Lian, T.; Gao, Q.; Nan-Xun, H.; Sironi, C. J Appl Polym Sci 1995, 57, 473.
9. Wu, D.; Chen, F.; Li, R.; Shi, Y. Macromolecules 1997, 30, 6737.
10. Mallon, F. K.; Ray, W. H. J Appl Polym Sci 1998, 69, 1233.
11. Chen, S.-A.; Chen, F.-L. J Polym Sci, Part A: Polym Chem 1987, 25, 533.
12. Ravindranath, K.; Mashelkar, R. A. J Appl Polym Sci 1990, 39, 1325.
13. Tate, S.; Ishimaru, F. Polymer 1995, 36, 353.
14. Huang, B.; Walsh, J. J. Polymer 1998, 39, 6991.
15. Mallon, F.; Beers, K.; Ives, A.; Ray, W. H. J Appl Polym Sci 1998, 69, 1789.
16. Tate, S.; Watanabe, Y.; Chiba, A. Polymer 1993, 34, 4974.
17. Parashar, M. K.; Gupta, R. P.; Jain, A.; Agarwal, U. S. J Appl Polym Sci 1998, 67, 1589.

18. Mallon, F. K.; Ray, W. H. J Appl Polym Sci 1998, 69, 1775.
19. Odian, G. Principles of Polymerization, 3rd ed.; Wiley & Sons: New York, 1991.
20. Buxbaum, L. H. J Appl Polym Sci Appl, Polym Symp 1979, 35, 59.
21. Jabarin, S. A.; Balduff, D. C. J Liq Chromatogr 1982, 5, 1825.
22. Radhakrishnan, S.; Iyer, V. S.; Sivaram, S. Polymer 1994, 35, 3789.
23. Dotson, N. A.; Galvan, R.; Laurence, R. L.; Tirrell, M. Polymerization Process Modeling; VCH Publishers: New York, 1996.
24. Hersh, S. N.; Choi, K. Y. J Appl Polym Sci 1990, 41, 1033.
25. Kim, Y.; Choi, K. Y.; Chamberlin, T. A. Ind Eng Chem Res 1992, 31, 2118.
26. Brunelle, D. J.; Boden, E. P.; Shannon, T. G. J Am Chem Soc 1990, 112, 2399.
27. Kim, Y.; Choi, K. Y. J Appl Polym Sci 1993, 49, 747.
28. Yoon, K. H.; Kwon, M. H.; Jeon, M. H.; Park, O. O. Polym J 1993, 25, 219.
29. Hulbert, H. M.; Katz, S. Chem Eng Sci 1964, 19, 555.
30. Tai, K.; Arai, Y.; Teranishi, H.; Tagawa, T. J Appl Polym Sci 1980, 25, 1789.
31. Grinsted, R. A.; Koenig, J. L. Macromolecules 1992, 25, 1229.
32. Goodner, M. D.; DeSimone, J. M.; Kiserow, D. J.; Roberts, G. W. Ind Eng Chem Res 2000, 39, 2797.
33. Lee, K. J.; Moon, D. Y.; Park, O. O.; Kang, Y. S. J Polym Sci, Part B: Polym Phys 1992, 30, 707.
34. Pell, T. M.; Davis, T. G. J Polym Sci, Part B: Polym Phys 1973, 11, 1671.
35. Rafler, G.; Bonatz, E.; Reinisch, G.; Gajewski, H.; Zacharias, K. Acta Polym 1980, 31, 732.
36. Schnell, H. Chemistry and Physics of Polycarbonates, 3rd ed.; Interscience Publishers: New York, 1964.